This is the accepted manuscript of the article that appeared in final form in **Surface and Coatings Technology** 321 : 484-490 (2017**)**, which has been published in final form at https://doi.org/10.1016/j.surfcoat.2017.05.013.

"Accelerated ageing of hybrid acrylic waterborne coatings containing metal oxide nanoparticles: effect on the microstructure"

Miren Aguirre[1], Monika Goikoetxea[2], Luis Alberto Otero[3], Maria Paulis[1], Jose R. Leiza[1]

[1]POLYMAT and Kimika Aplikatua Saila, Kimika Zientzien Fakultatea, University of the Basque Country UPV/EHU, Joxe Mari Korta Zentroa, Tolosa Hiribidea 72, 20018 Donostia-San Sebastián, Spain

[2]Nanooptics Group, CIC nanoGUNE Consolider, 20018 Donostia-San Sebastián, Spain

[3]Foresa, R&D Department, Avda. Doña Urraca, 91, 36650 Caldas de Reis, Pontevedra, Spain

Abstract

This work analyses the effect of UV irradiation in a pure acrylic film, and two hybrid films, one with 1% CeO_2 nanoparticles and another with 1 % of ZnO nanoparticles. The long term durability of the polymeric films was studied by accelerated UV exposure ageing. The changes occurring in the polymeric films were analyzed by measuring thermal properties, molecular weight distributions (MWD), formation of cross-linked or gel structures and the morphology by Transmission Electron Microscopy (TEM). The results revealed small changes (almost negligible) in the thermal properties and morphology whereas some differences were found when the microstructure was analyzed. Nevertheless, these differences were similar in the three studied films, discarding any additional degradation effect of CeO_2 and ZnO nanoparticles on acrylic films.

Highlights

- Accelerated UV exposure tests of bare acrylic/metal oxide (CeO_2 or ZnO) hybrid coatings have been carried out.
- The UV exposure affects to the microstructure of the hybrid metal oxide coatings as well as to the blank acrylic coating.
- Concerns about the photocatalytic ability of CeO_2 and ZnO nanoparticles in acrylic coatings have been clarified.

Key-words: accelerated exposure, UV radiation, CeO_2 and ZnO nanoparticles, and acrylic hybrid films.

1. Introduction

The UV light, ranging from 250 to 400 nm, represents about 5% of the total irradiation reaching the earth's surface. UV radiation has detrimental effects on surfaces such as metal, glass, wood or human skin. All these surfaces can be protected against radiation with polymer coatings. Precisely, waterborne acrylic polymers are widely used in the formulation of varnishes and paints as protective coatings for different surfaces due to their low toxicity and good quality film forming properties[1]. Nevertheless, a common failure in outdoor acrylic coatings applications is the photodegradation due to UV exposure, which causes structural changes and the consequent variation of the overall coating properties[2]. Though the polymer itself is non toxic and durable in outer environment, incorporation of UV absorbers and Hindered Amine Light Stabilizers (HALS) is necessary to increase the lifetime and improve the properties of the coating[3]. Therefore, due to the increasing pressure of the environmental legislation to reduce the volatile organic contents (VOC) the use of non toxic UV absorbers, such as metal oxides, has increased considerably[4]. Titanium oxide (TiO_2), zinc oxide (ZnO) and cerium oxide (CeO_2) are widely used to block the solar radiation and to reduce the speed of photodegradation processes of the surfaces due to their broad UV spectrum attenuation properties and also their stability under radiation[5–9].

Nevertheless, it should be taken into consideration the photocatalytic activity of those metal oxides. TiO_2, CeO_2 and ZnO have almost the same band gap energy (3.0-3.4 eV), and share the same UV absorption mechanism, under UV light the molecules get excited by absorbing a photon which creates an electron-hole pair. In the case of TiO_2 nanoparticles, these electron-hole pairs migrate to the surface of the particles and eventually react with oxygen, water or hydroxyls to form free radicals. This process is known as photocatalysis and it has been used to develop self-cleaning and antibacterial coatings and paints[10–12]. On the contrary, it has been

proved that the photocatalytic activity of the CeO_2 and ZnO nanoparticles is lower than that of the TiO_2[13]. Consequently, CeO_2 and ZnO seem to be good candidates due to their low photocatalytic activity to use as UV blocking material.

In our previous studies, it was reported the synthesis of high solids content acrylic/CeO_2[8,14] and acrylic/ZnO[9] hybrid latexes to use as UV blocking binders. Those latexes were obtained by a two step polymerization process which led to encapsulation of the nanoparticles into acrylic polymer particles. The main advantage of having the nanofillers encapsulated inside the polymer particles was the lack of aggregation during film formation and leaching from the polymeric film. Therefore, good quality and transparent polymeric films were obtained with excellent UV absorption capacity. However, concerns were raised (at conferences and during publication procedure by reviewers) on the potential photodegradability of the coating matrix due to the photocatalytic or redox activity of the CeO_2 and ZnO used. This analysis was out of the scope of these papers, and it is the main objective of this work.

Photodegradation of hybrid acrylic coatings have been reported in the literature but in most of the cases the coatings were tested in substrates such as glass, stone or wood.[2,6,7,15] For instance, in the case of wood, lignin strongly absorbs in the UV-Vis region which leads to different chemical reactions and thus to photodegradation of the wood surface[16]. So once the UV light reaches the wood surface, formation of free radicals starts. Hence, there might be two sources of generation of radicals; one coming from the substrate itself and the other one from the metal oxides present in the hybrid acrylic films. In order to solve these concerns and to clarify the effect that the metal oxide nanoparticles have during photodegradation of acrylic binders, the degradation behavior of bare acrylic films was performed in this work.

Therefore, the objective of the present work was to analyze the effect that long exposure times to UV radition of bare acrylic/CeO_2, acrylic/ZnO and pure acrylic polymeric films have on their microstructure and properties. Accelerated ageing test was used to assess the performance of the newly developed coatings.

2. Materials and methods

The acrylic polymer latexes containing 1% of CeO_2, 1% of ZnO and without inorganic nanoparticles were synthesized by seeded semibatch emulsion polymerization according to the procedure already described elsewhere[8,9]. The composition, the solids content, the average particle sizes and the polydispersity index of the latexes are presented in Table 1. The particles sizes were measured by Dynamic Light Scattering (DLS) using a Zetasizer Nano Series (Malvern Instrument).

Table 1. Solids content (SC), average particle size (Dp), polydispersity index (PDI) and monomer composition of the three different latexes used to produce the films.

	SC (%)	Dp (nm)	PDI	MMA wt%	BA wt%	AA wt%
Blank	38	145	0.009	49.5	49.5	1
1% CeO_2	40	173	0.021	49.5	49.5	1
1% ZnO	42	392	0.038	50	50	-

Five films (20 x 5 x 0.12 mm) were casted in Teflon molds for each polymer latex at room temperature. Four of these films were exposed to accelerated weathering test and the fifth one was kept as reference.

Accelerated weathering test was conducted in a SolarBox 1500 with a Xenon lamp of 1500W (UVA irradiation) and having a constant irradiation at a power of 770 W/m^2. All the above mentioned samples were exposed to UV light for different time spans with maximum exposure time of 3200 h. Therefore, a sample for each coating was taken out of the SolarBox after 800 h, 1600 h, 2400 h and 3200 h of exposure.

The glass transition temperature (Tg) was measured by Differential Scanning Calorimetry (DSC) in a Q2000, TA Instruments. The samples were cooled to -50 °C and then the analysis started by

heating up to 150 °C at 10 °C/min; 2 cycles were completed for each sample. The reported Tgs correspond to the second cycle.

Thermogravimetric analysis (TGA) was performed to the coatings in a Q500, TA Instruments. The samples were heated from 0 to 800 °C with a heating rate of 10 °C/min under nitrogen atmosphere.

The gel fractions of the samples were measured via conventional Soxhlet extraction, using technical grade tetrahydrofuran (THF) as solvent. Molecular weight distributions of the soluble part were determined by Size Exclusion Chromatography (SEC). The samples were dried at room temperature and dissolved in THF. The solutions were filtered (polyamide 0.45 µm) before injection into the GPC, which consisted of a pump (Shimadzu LC-20AD), three columns (Styragel HR2, HR4 and HR6) and a refractive index detector (Waters 2410). Chromatograms were obtained at 35 °C using a THF flow rate of 1 mL/min.

For the Infrared (IR) analysis, a Bruker Hyperion 2000 microscope coupled to a Vertex 70 Fourier Transform Infrared Spectroscopy (FTIR) spectrometer was used, equipped with Attenuated Total Reflectance (ATR) module and a liquid-nitrogen-cooled mid-band mercury cadmium telluride detector. The ATR module (20X ATR objective, single internal reflection) comprised a germanium crystal with a diameter of about 100 mm at the point of contact with the sample and integrated pressure sensor. The spectra were measured with a spectral resolution of 4 cm^{-1} and present an average over 250 scans.

The morphology of the films was analyzed by Transmission Electron Microscopy (TEM), TECNAI G2 20 TWIN (FEI), operating at an accelerating voltage of 200 keV in a bright field image mode. The films were trimmed at -40 °C using an ultramicrotome device (Leica EMFC6) equipped with a diamond knife. The ultrathin sections (100 nm) were placed on 300 mesh copper grids. Nanoparticles size distributions were obtained using Image Pro Plus 7.0 software counting 500 nanoparticles of each kind.

3. Results and Discussion

As it can be seen in Figure 1 the bare blank and the hybrid containing 1% of ZnO nanoparticles were totally transparent before starting the test, whereas the film containing 1% of CeO_2 nanoparticles was slightly yellowish. Nonetheless, as shown in Figure 1, during the exposure time the neat acrylic film became yellowish and the color increased slightly in the film containing nanoceria, while the transparency and lack of color in the film containing ZnO nanoparticles was maintained. Besides, by Scanning Electron Microscopy (SEM) it was seen that the surfaces of the films did not present any damage or cracking during the exposure (images not shown here).

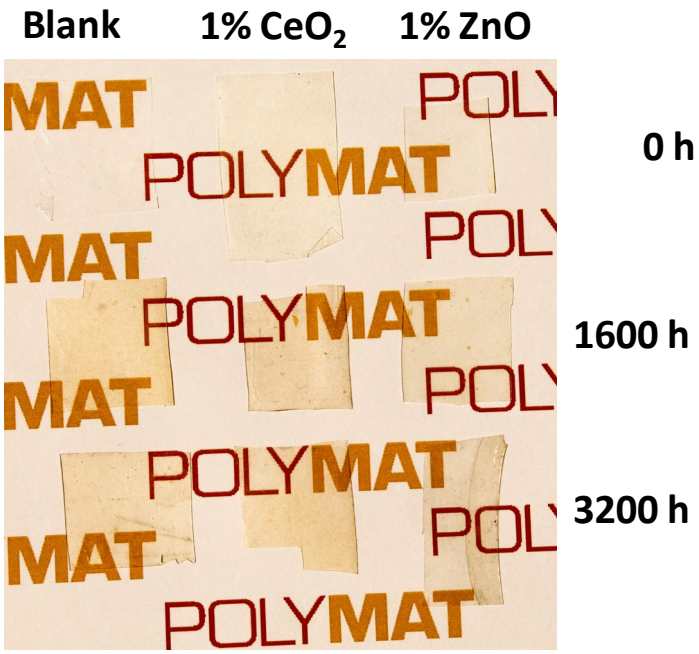

Figure 1. Films appearance before starting the accelerated test, after 1600 h and after 3200 h of UV radiation exposure.

The thermal properties of the neat acrylic coating and coatings containing 1 wt% of CeO_2 and ZnO nanoparticles were analyzed using DSC and TGA curves. Table 2 and Figure 2 present the average values and the standard deviations of the Tg and DSC curves of the acrylic films after different periods of time in the UV chamber, two measurements were carried out for each sample. It can be seen that the Tg was only slightly altered during the UV exposure; an increase

of 1 or 2 °C was observed in all cases. The Tg after 3200h of exposure was of 21°C while for the 1% CeO_2 and 1% ZnO films were of 18 °C and 16 °C respectively. The Tg slightly decreased with the addition of the nanoparticles, being the decrease more pronounced for the ZnO hybrid, likely due to larger sizes of the ZnO aggregates[9] (see Figure 7) in the acrylic matrix that increased the free volume. This trend was maintained after the UV radiation exposure.

Table 2. Glass transition temperatures for the films after different accelerated UV exposure times.

	Before	After 1600 h	After 2400 h	After 3200 h
Blank	20±1 °C	21±1 °C	22±1 °C	21±0 °C
CeO_2	17±0 °C	17±1 °C	17±1 °C	19±1 °C
ZnO	15±1.5 °C	16±0 °C	16±1 °C	17±1 °C

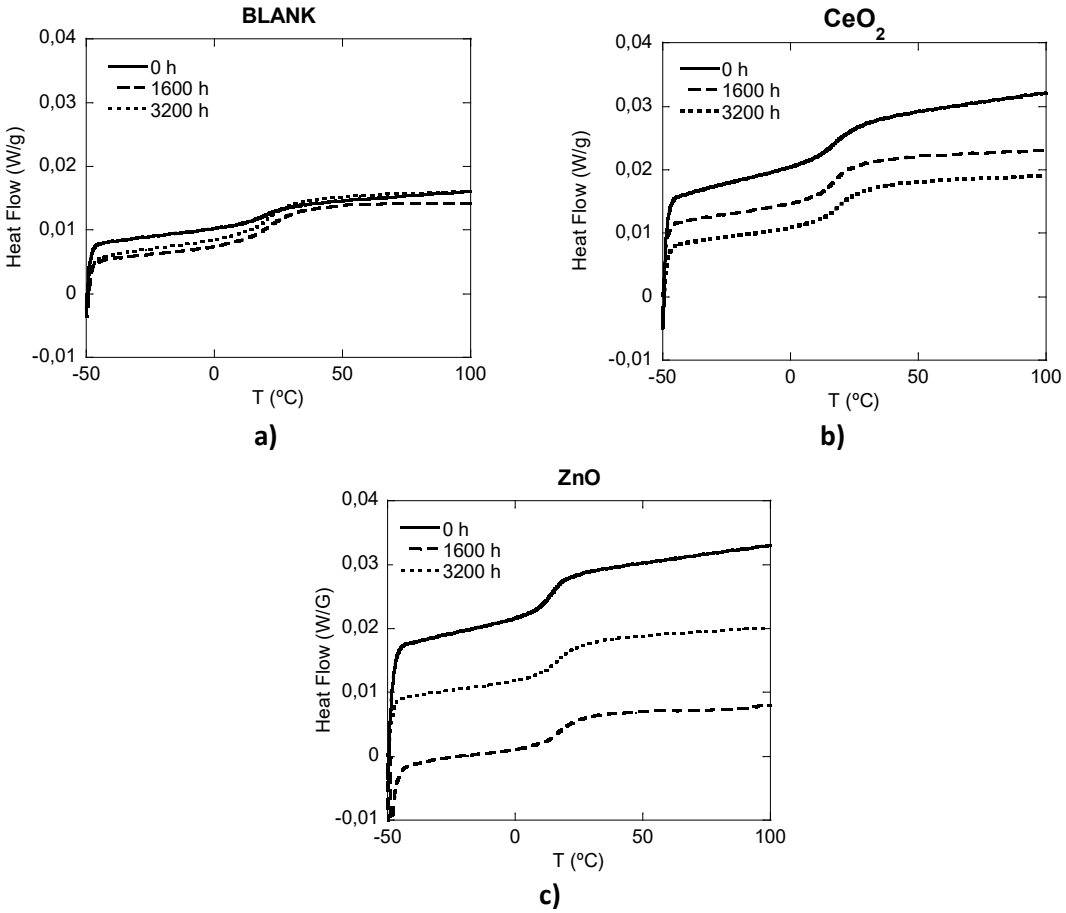

Figure 2. DSC curves for a) Blank films, b) film containing 1 wt% of CeO_2 nanoparticles and c) film containing 1 wt% of ZnO nanoparticles after different accelerated UV exposure times.

The TGA curves for the three samples before and after 3200 h of exposure are plotted in Figure 3. The curves exhibit one step thermal degradation process, being the decomposition temperature around 380 °C in all of them. The decomposition temperature values are in good agreement with those found in the literature for pure acrylic binders[17]. These results revealed that there was no effect on the thermal properties of the coatings with the addition of the metal oxide nanoparticles and that the degradation pathway was not affected by the presence of the inorganic nanoparticles. Although the films containing nanoparticles should present larger residual weight amount, due to the small amount of them (1 wt% with respect to the polymer) it could hardly be detected.

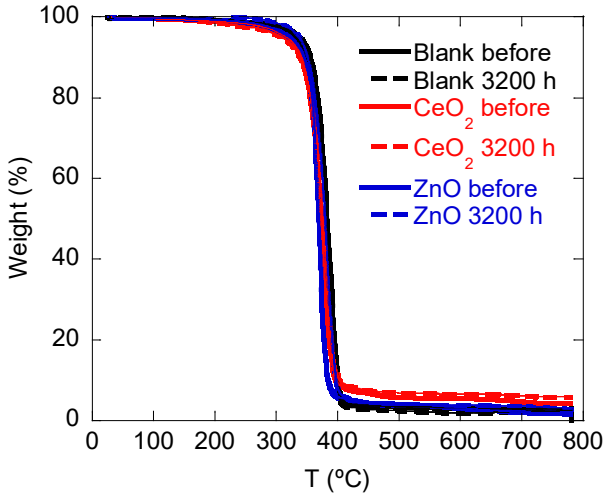

Figure 3. TGA curves for the polymeric films before and after the UV radiation exposure.

The molecular weight and molecular weight distribution (MWD) of the soluble fraction of the films was measured by Size Exclusion Chromatography (SEC). It can be seen in Table 3 that the average molecular weight of the soluble part decreased when increasing the UV exposure time. In order to shed light on the reasons for this decrease the SEC traces were analyzed (Figure 4). The molecular weight distribution did not show any visible tailing towards low molecular weights, which means that cleavage of the chains or formation of side products during UV exposure did not occur. The minimum value of the MWD was maintained whereas the larger values shifted to lower Mw. These results are in good agreement with the TGA curves, in which the presence of side products or different degradation pathways was not observed.

Table 3. Weight average molecular weights for the three polymeric coatings at different accelerated UV exposure times.

	Mw (KDa) Before	Mw (KDa) 800h	Mw (KDa) 1600h	Mw (KDa) 3200h
Blank	198.5	184.1	108.6	90.2
CeO_2	226.2	140.4	113.0	73.9
ZnO	338.4	327.7	206.1	207.5

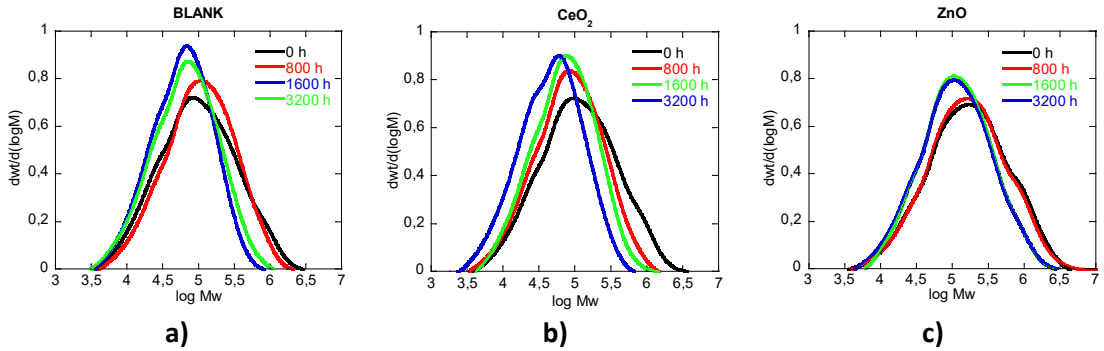

Figure 4. Molecular weight distribution (MWD) of the soluble part of the a) blank film, b) 1% CeO_2 hybrid film and c) 1% ZnO hybrid film after different UV exposure time.

On the other hand, this decrease in the molecular weight of the soluble part could be related to the formation of cross-linked structures which are not soluble in THF that preferentially incorporate the larger polymer chains[18,19]. This is true in the polymerization of acrylates and it has also been observed during accelerated exposure by Lazzari et al. [2] that they associated this effect to degradation processes occurring in BA units, since a common degradation pathway of meth(acrylic) polymers containing long alkyd side-groups is the formation of cross-linked polymer structures.

Taking these ideas into consideration, the THF insoluble fraction of the films was measured by Soxhlet extraction. In the results shown in Table 4, it can be seen that the insoluble part related to the cross-linked structures increased with the UV exposure time.

Table 4. THF insoluble part in percentage measured by Soxhlet Extraction for the three different films.

	0 h	800 h	1600 h	3200 h
Blank	46	48	63	58
CeO_2	69	56	59	94
ZnO	35	30	46	40

*Reproducibility of the measurements was not carried out because of the small amount of sample. For similar samples the error associated with the measurements was between 2-3%[8].

Therefore, degradation in the microstructure of the films was observed during the UV radiation, even if no additional effect was found in the presence of the nanoparticles.

The sol Mw and gel content of the films affected the mechanical properties of the film. The mechanical properties are commonly measured by stress-strain measurements. Unfortunately, the film specimens tested in this work in the accelerated ageing were too small to get standard probes (e.g. ASTM D882). Tensile test were carried out with smaller probes but it was not possible to obtain meaningful results. Alternatively, we tried to use PeakForce Quantitative Nanomechanical Mapping (QNM), since it has been shown that this technique can provide the mechanical properties of polymeric films[20,21] without the need of large amount of material to be analyzed. The surface modulus of the films tested were too small compared with the materials used to calibrate the equipment[22] and hence, we could not analyze the effect that ageing had on the mechanical properties of the films, neither correlate the changes in the MWD with these properties.

It has been reported that the most remarkable changes in FTIR during degradation of (metha)acrylate films, is the increase in the absorption of the hydroxyl region, between 3400 cm^{-1} and 3200 cm^{-1}, which is caused by oxidation reactions. This effect appears together with the decrease and broadening of the carbonyl peak at 1730 cm^{-1} and a simultaneous formation of a new component of the carboxyl group at a larger wavelengths of around 1780 cm^{-1} [2,16,23]. Figure 5 shows the ATR-FTIR spectra of the neat acrylic and the coatings containing 1 wt% of

CeO_2 and ZnO nanoparticles, before and after 1600 h and 3200 h of UV exposure. Contrary to what has been reported, the changes observed after the UV exposure are not significant in any of the samples measured in this work. It was not possible to detect neither the formation of hydroxyl groups nor alterations in the carboxyl peak region. It should be mentioned that the data was normalized, but no further treatment was done. The differences in the relative intensities might be related to the irreproducibility between ATR measurements. The main differences were found above 3500 cm^{-1} which could be related to the noise (there is no clear trend in the three samples) whereas the peaks below 1000 cm^{-1} are vibrations between the metal and oxygen[24]. Furthermore, the addition of CeO_2 or ZnO nanoparticles did not alter this lack of degradation sings that the blank film presented.

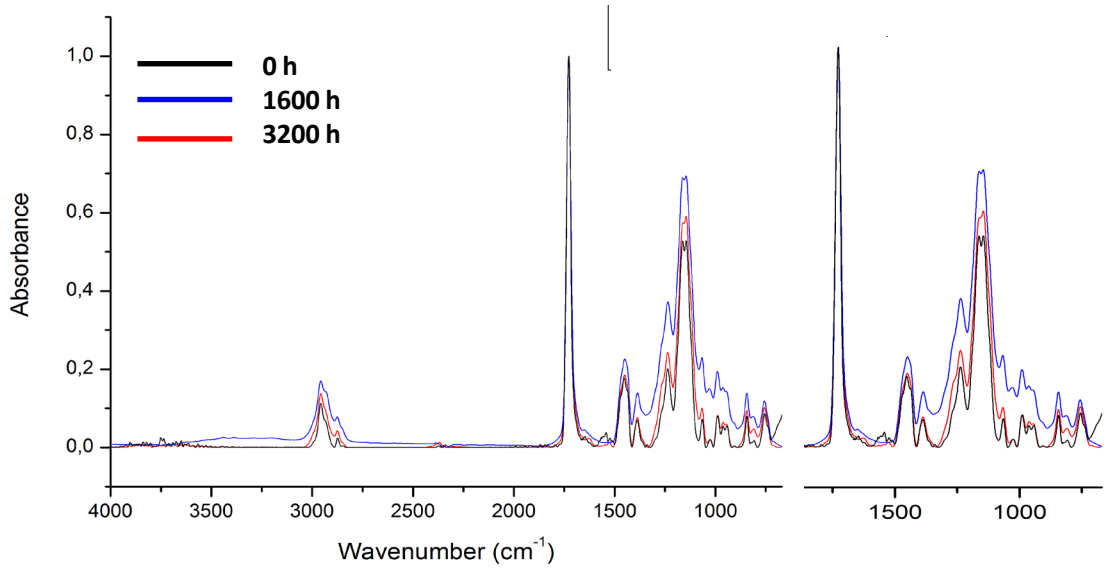

a)

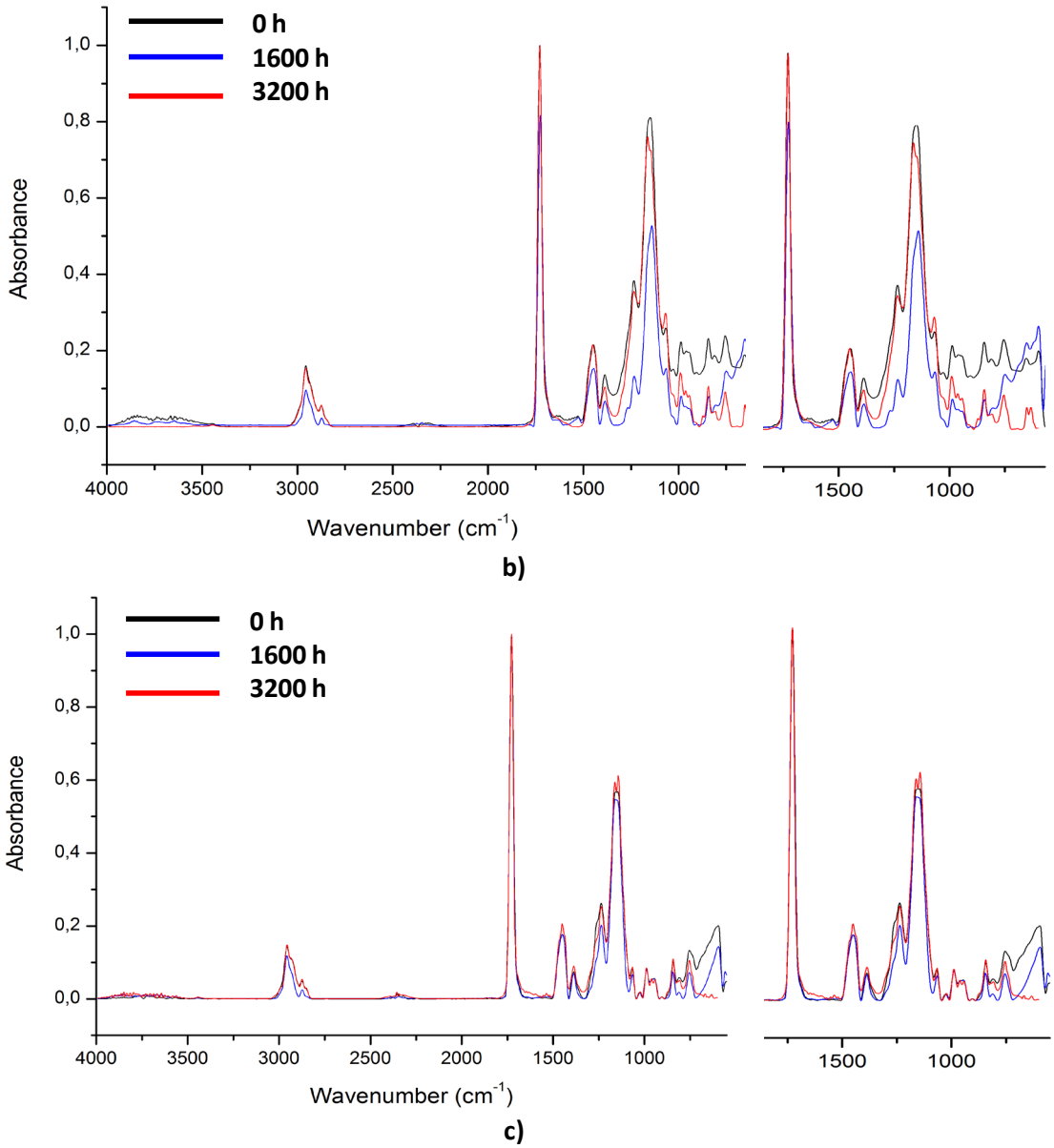

Figure 5. ATR-FTIR spectra and magnifications for a) blank film, b) 1% CeO_2 film and c) 1% ZnO films at 0 h, 1600 h and 3200 h of UV exposure.

A potential explanation of the small differences found in the ATR-FTIR spectra in this study, could be found in the higher thickness of the films tested in this work (the thickness of the films was higher than 120 µm). The thicker the film, the more degradation is needed to detect side products by ATR-FTIR spectroscopy, since the overall concentration of the newly formed products is smaller. The thickness of this type of binders when they are applied as coatings is normally around 100 µm, which means that during their natural exposure time, they will not suffer any drastic change after 3200 h of exposure as it has been demonstrated in this work.

Another concern regarding those metal oxide hybrid films was whether the aggregation and/or the detachment of the inorganic nanoparticle from the polymer matrix could occur upon ageing. This can lead to leaching of the metal oxide nanoparticles during their outdoor exposure. To address this issue, the hybrid films after 3200 h of irradiation were analyzed by TEM and the average size of the nanoparticles aggregates and their distributions were determined. In our previous studies, it was observed that the distribution of the CeO_2 nanoparticles in the polymeric films was very homogeneous and that there was not aggregation of the nanoparticles during film formation[8]. Figure 6 presents the TEM micrographs and the aggregate size distributions calculated from them. Qualitatively no substantial difference can be observed in the TEM micrographs of the films before and after UV exposure. In both cases nanoparticles between 3 and 73 nm were found and the calculated volume average aggregate size was 24 nm for both films. This demonstrates that there was not aggregation neither detachment of the CeO_2 nanoparticles during the UV exposure of the film.

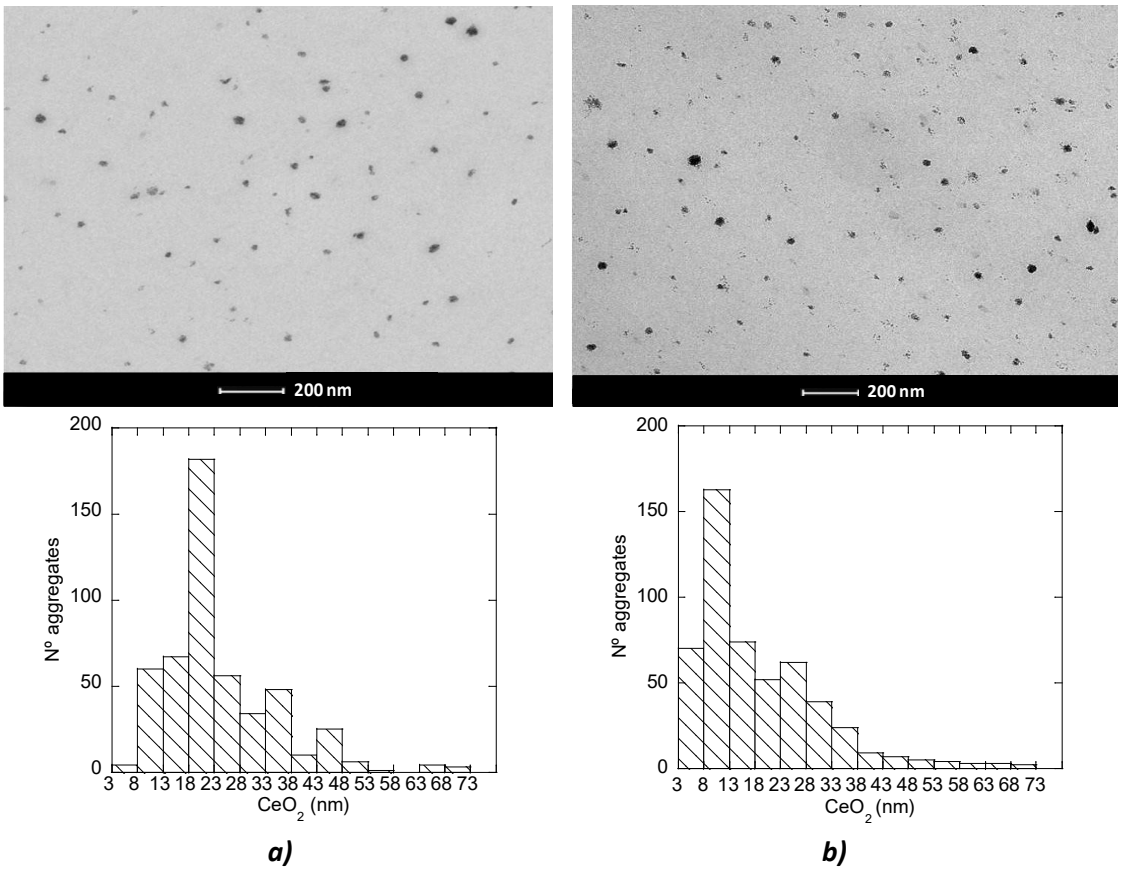

Figure 6. TEM micrographfor a 1% CeO_2 hybrid film and CeO_2 nanoparticle's size distribution a) before UV exposure and b) after 3200 h of UV exposure.

In the case of the hybrid films containing ZnO nanoparticles, the size of the ZnO domains was bigger as shown in our previous work[9]. Nevertheless, as shown in Figure 7, the exposure to UV did not produce further aggregation of the ZnO domains (between 25 and 800 nm in size) found before exposure. The calculated volume average aggregate size was 190 nm before the exposure and 178 nm after the UV exposure. It can be concluded that the encapsulated morphology of CeO_2 and ZnO nanopartices in the latex particles, prevented their aggregation during film formation, and favored the preservation of the homogeneous distribution of the nanoparticles in the films after UV exposure.

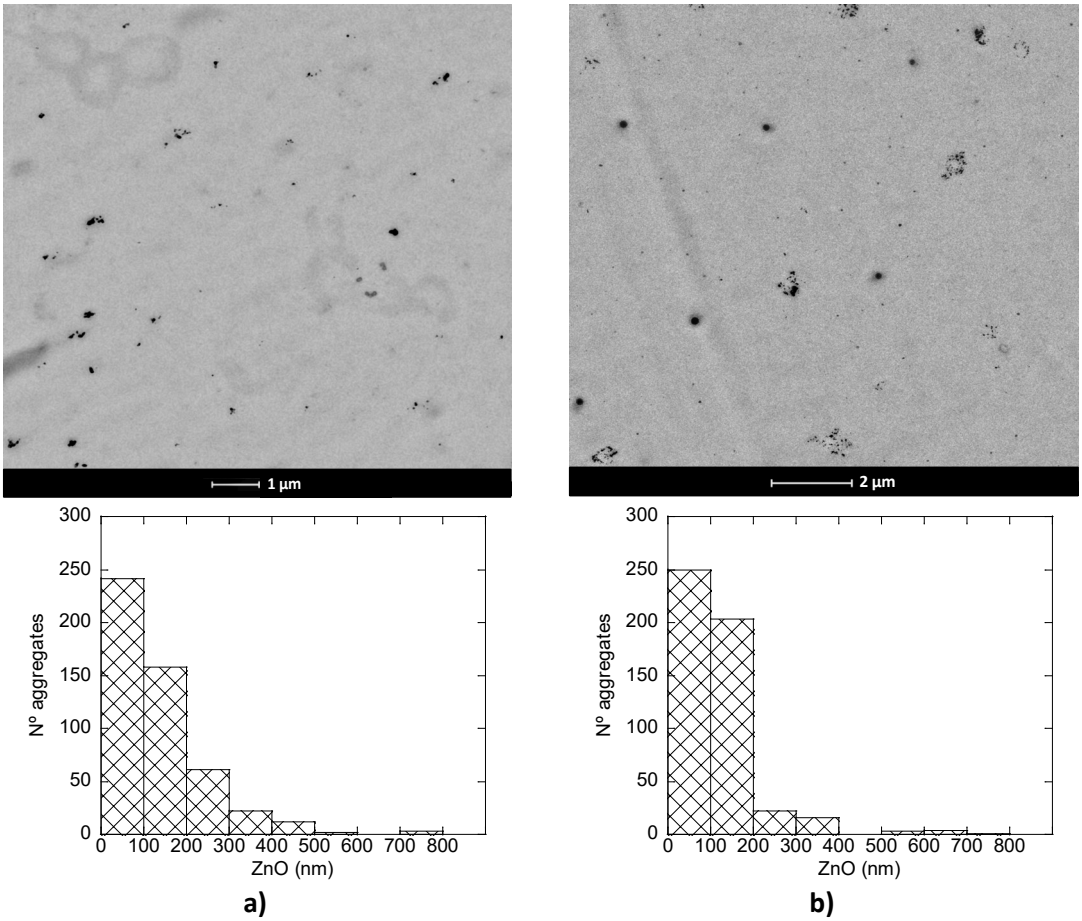

Figure 7. 1% ZnO film TEM micrograph and nanoparticle's size distribution a) before UV exposure and b) after 3200h of UV exposure.

4. Conclusions

The photodegradation of three different acrylic films namely, a pure acrylic film, a film containing 1% of CeO_2 nanoparticles and another containing 1% of ZnO was studied by

accelerated UV exposure test. It was possible to detect some microstructural changes in the film, even if it did not affect either the thermal properties or the morphology of the polymeric matrix. The concerns about the possible photoactivity and the acceleration of the photodegradation that the metal oxide nanoparticles could produce in acrylic binders have been discarded, owing to the similar properties obtained for the pure acrylic film and the ones containing 1% CeO_2 and 1% ZnO of nanoparticles.

Acknowledgements

Miren Aguirre thanks the financial support given by the European Union (Woodlife project FP7-NMP-2009-SMALL-246434), the UPV/EHU "Doktore berriak kontratatzeko eta horiek doktorego ondoko prestakuntza programetan sartzeko laguntza" and also the financial support received from Ministerio de Economía y Competitividad de España, Juan de la Cierva en Formación (FJCI-2014-22336). The sGIKer UPV/EHU is acknowledged for the electron microscopy facilities of TEM. FORESA is gratefully acknowledged for the Accelerated UV trials in the Solar Box 1500.

BIBLIOGRAPHY

1. Katangur P, Patra PK, Warner SB. Nanostructured ultraviolet resistant polymer coatings. *Polym Degrad Stab*. 2006;91:2437-2442. doi:10.1016/j.polymdegradstab.2006.03.018.
2. Lazzari M, Scalarone D, Malucelli G, Chiantore O. Durability of acrylic films from commercial aqueous dispersion: Glass transition temperature and tensile behavior as indexes of photooxidative degradation. *Prog Org Coatings*. 2011;70(2-3):116-121. doi:10.1016/j.porgcoat.2010.11.002.
3. Ammala A, Hill AJ, Meakin P, Pas SJ, Turney TW. Degradation studies of polyolefins incorporating transparent nanoparticulate zinc oxide UV stabilizers. *J Nanoparticle Res*. 2002;4:167-174.
4. Schaller C, Rogez D, Braig A. Organic vs inorganic light stabilizers for waterborne clear coats: a fair comparison. *J Coatings Technol Res*. 2011;9(4):433-441. doi:10.1007/s11998-011-9380-8.
5. Vlad M, Riedl B, Blanchet P. Enhancing the performance of exterior waterborne

coatings for wood by inorganic nanosized UV absorbers. *Prog Org Coatings*. 2010;69(4):432-441. doi:10.1016/j.porgcoat.2010.08.006.

6. Saha S, Kocaefe D, Boluk Y, Pichette A. Surface degradation of CeO2 stabilized acrylic polyurethane coated thermally treated jack pine during accelerated weathering. *Appl Surf Sci*. 2013;276:86-94. doi:10.1016/j.apsusc.2013.03.031.

7. Saha S, Kocaefe D, Krause C, Larouche T. Effect of titania and zinc oxide particles on acrylic polyurethane coating performance. *Prog Org Coatings*. 2011;70:170-177. doi:10.1016/j.porgcoat.2010.09.021.

8. Aguirre M, Paulis M, Leiza JR. UV screening clear coats based on encapsulated CeO2 hybrid latexes. *J Mater Chem A*. 2013;1(9):3155-3162. doi:10.1039/c2ta00762b.

9. Aguirre M, Barrado M, Iturrondobeitia M, et al. Film forming hybrid acrylic/ZnO latexes with excellent UV absorption capacity. *Chem Eng J*. 2015;270:300-308. doi:10.1016/j.cej.2015.02.025.

10. González E, Bonnefond A, Barrado M, Casado AM, Asua JM, Leiza JR. Photoactive self-cleaning polymer coatings by TiO 2 nanoparticle Pickering miniemulsion polymerization. *Chem Eng J*. 2015;281:209-217. doi:10.1016/j.cej.2015.06.074.

11. Bonnefond A, González E, Asua JM, et al. Biointerfaces New evidence for hybrid acrylic / TiO 2 films inducing bacterial inactivation under low intensity simulated sunlight. *Colloids surfaces B Biointerfaces*. 2015;135:1-7.

12. Parkin IP, Palgrave RG. Self-cleaning coatings. *J Mater Chem*. 2005;15:1689-1695. doi:10.1039/b412803f.

13. Bennett SW, Keller AA. Comparative photoactivity of CeO2, γ-Fe2O3, TiO2 and ZnO in various aqueous systems. *Appl Catal B Environ*. 2011;102(3-4):600-607. doi:10.1016/j.apcatb.2010.12.045.

14. Aguirre M, Paulis M, Leiza JR, et al. High-Solids-Content Hybrid Acrylic/CeO2 Latexes with Encapsulated Morphology Assessed by 3D-TEM. *Macromol Chem Phys*. 2013;214:2157-2164.

15. Serra CL, Tulliani JM, Sangermano M. An Acrylic Latex Filled with Zinc Oxide by Miniemulsion Polymerization as a Protective Coating for Stones. *Macromol Mater Eng*. 2014;299:1352-1361. doi:10.1002/mame.201400074.

16. Forsthuber B, Grüll G. The effects of HALS in the prevention of photo-degradation of acrylic clear topcoats and wooden surfaces. *Polym Degrad Stab*. 2010;95:746-755. doi:10.1016/j.polymdegradstab.2010.02.016.

17. Topçuoğlu Ö, Altinkaya SA, Balköse D. Characterization of waterborne acrylic based paint films and measurement of their water vapor permeabilities. *Prog Org Coatings*. 2006;56(4):269-278. doi:10.1016/j.porgcoat.2006.02.003.

18. Hamzehlou S, Ballard N, Carretero P, et al. Mechanistic investigation of the simultaneous addition and free- radical polymerization in batch miniemulsion droplets : Monte Carlo simulation versus experimental data in polyurethane / acrylic systems. *Polymer (Guildf)*. 2014;55(19):4801-4811. doi:10.1016/j.polymer.2014.07.024.

19. Arzamendi G, Leiza JR. Molecular Weight Distribution (Soluble and Insoluble Fraction) in Emulsion Polymerization of Acrylate Monomers by Monte Carlo Simulations. *Ind Eng Chem Res*. 2008;47:5934-5947.

20. Dokukin ME, Sokolov I. Quantitative Mapping of the Elastic Modulus of Soft Materials with HarmoniX and PeakForce QNM AFM Modes. *Lagmuir*. 2012;28:16060-16071.

21. Cheng X, Putz KW, Wood CD, Brinson LC. Characterization of Local Elastic Modulus in Confi ned Polymer Films via AFM Indentation. *Macromol Rapid Commun*. 2015;36:391-397.

22. Young TJ, Monclus MA, Burnett TL, Broughton WR, Ogin SL, Smith PA. The use of the PeakForce TM quantitative nanomechanical mapping AFM-based method for high-resolution Young's. *Meas Sci Technol*. 2011;22(125703):1-6. doi:10.1088/0957-0233/22/12/125703.

23. Chiantore O, Trossarelli L, Lazzari M. Photooxidative degradation of acrylic and methacrylic polymers. *Polymer (Guildf)*. 2000;41:1657-1668.

24. Xiong M, Gu G, You B, Wu L. Preparation and Characterization of Poly(styrene butylacrylate) Latex Nano-ZnO Nanocomposites. *J Appl Polym Sci*. 2003;90:1923-1931.